METASURFACE INTEGRATED PATCH ANTENNA

By:

PRATHAM CHAKRABORTY(B222035)

ABSTRACT

This project focuses on the design and simulation of a metasurface-integrated inset-fed microstrip patch antenna for wireless communication applications. The antenna is built using a standard FR4 substrate and incorporates a specially engineered metasurface composed of copper ring structures. A controlled air gap is introduced between the patch and the metasurface layer to enhance electromagnetic interaction and reduce substrate losses. The metasurface modifies the effective permittivity and permeability around the patch, leading to improved impedance matching, bandwidth, and radiation characteristics. CST Studio Suite is used for simulating and optimizing the antenna structure. The design aims to overcome the common limitations of patch antennas, such as low gain and narrow bandwidth. The antenna maintains a low-profile, compact structure, making it suitable for integration in modern wireless systems. The study highlights how passive metasurface layers can significantly improve antenna performance without increasing complexity. This approach can be adapted for use in various applications such as Wi-Fi, IoT, and Bluetooth-enabled devices.

SPECIFICATIONS

- An inset-fed Microstrip Patch Antenna (MPA) is initially designed for operation at 2.4 GHz.
- The antenna is built on FR4 lossy material with a relative permittivity of 4.3 is used as the substrate.
- A full copper layer beneath the substrate functions as the ground plane.
- The patch radiator made of copper is positioned on top of the substrate.
- An inset-fed microstrip transmission line is employed to provide 50-ohm impedance matching.
- The rings of the metasurface are built on FR4 lossy material, which is being used as a substrate.
- The rings are made of copper.
- The ground plane beneath the metasurface is also made up of copper.

GEOMETRY

MICROSTRIP PATCH ANTENNA

MICROSTRIP FRONT

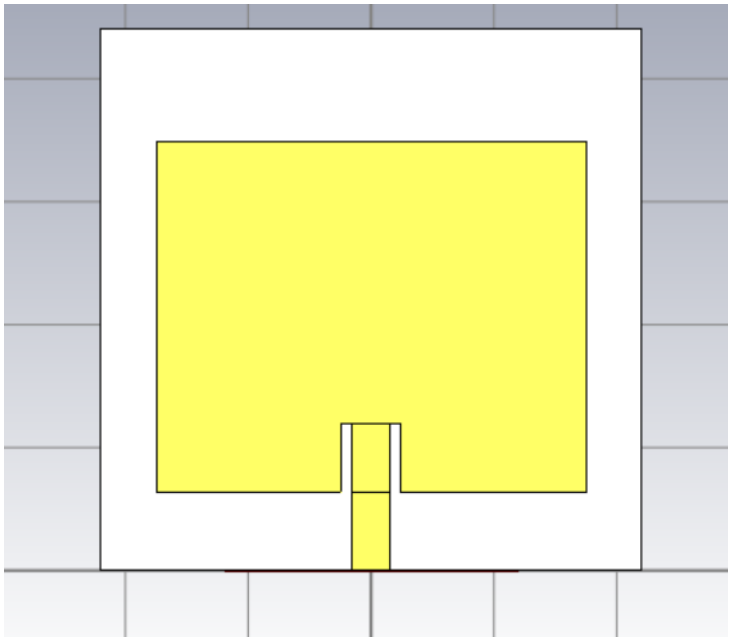

MICROSTRIP BACK

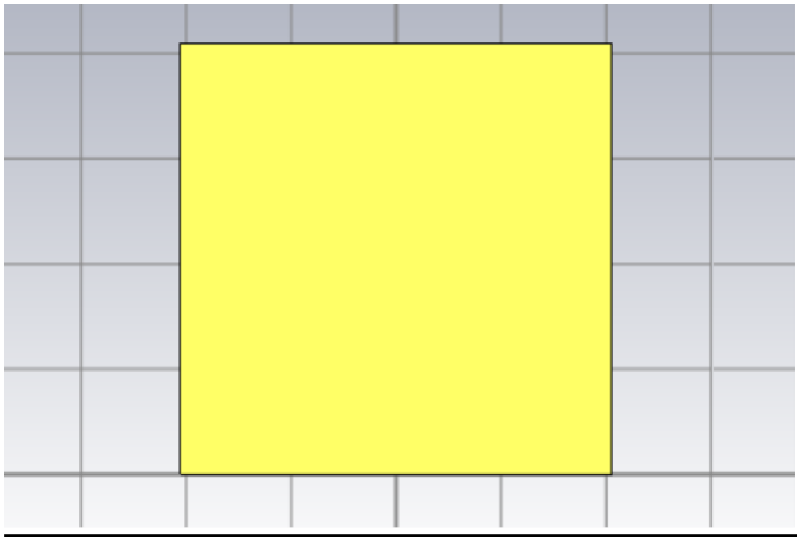

- **Substrate:**
    - Material: FR4 (lossy)
    - Thickness: 1.6 mm
    - Relative permittivity (εr): 4.3
    - Shape: Square
    - Size: 44 mm × 44 mm
- **Ground Plane:**
    - Material: Copper
    - Location: Full copper layer beneath the substrate
    - Thickness: 0.035mm
    - Size: 44 mm × 44 mm
- **Patch Radiator:**
    - Dimensions: 28.53 mm (Length) × 34.93 mm (Width)
    - Placement: On top of the substrate
    - Thickness: 0.035 mm
- **Feed Line:**
    - Dimensions: 12 mm x 3 mm
    - Thickness: 0.035 mm
    - Impedance: 50 Ohms
- **Inside Feed:**
    - Dimension: 5.65 mm x 0.9 mm

- There is an air gap of **0.5 mm** between the microstrip patch and the metasurface.

METASURFACE UNIT CELL GEOMETRY

METASURFACE UNIT CELL

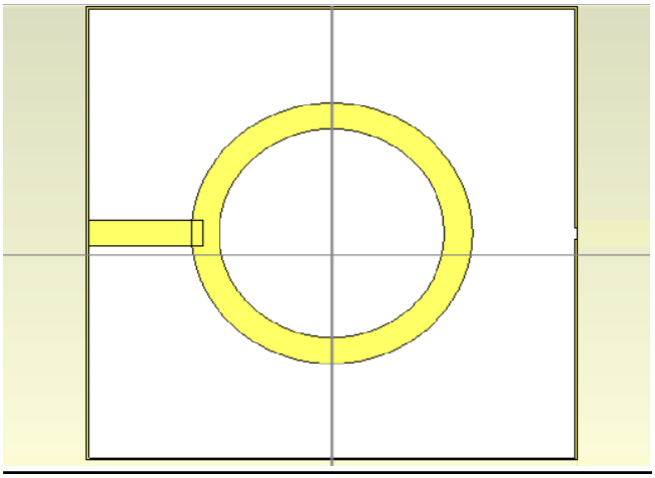

METASURFACE FRONT

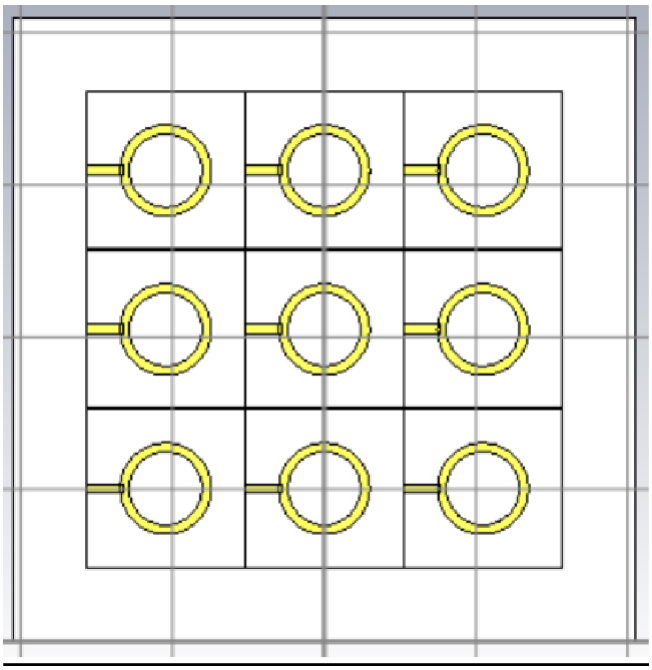

METASURFACE BACK

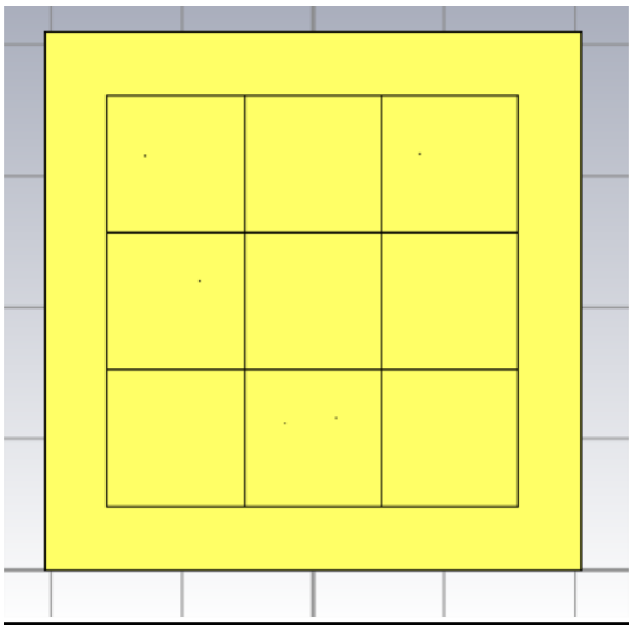

- **Substrate**:
  - Dimension: 10.45 mm x 10.45 mm
  - Thickness: 1.6 mm

- **Ground**:
  - Dimension: 10.45 mm x 10.45 mm
  - Thickness: 0.035 mm

- **AMC Patch:**
  - Dimension: 10.35mm x 0.1 mm
  - Thickness: 0.035 mm

- **Circular Patch:**
  - Inner Radius: 2.4 mm
  - Outer Radius: 3 mm
  - Thickness: 0.035 mm

- **Feedline:**
    - Dimension: 2.4 mm X 0.4 mm
    - Thickness: 0.035 mm

FULL ANTENNA

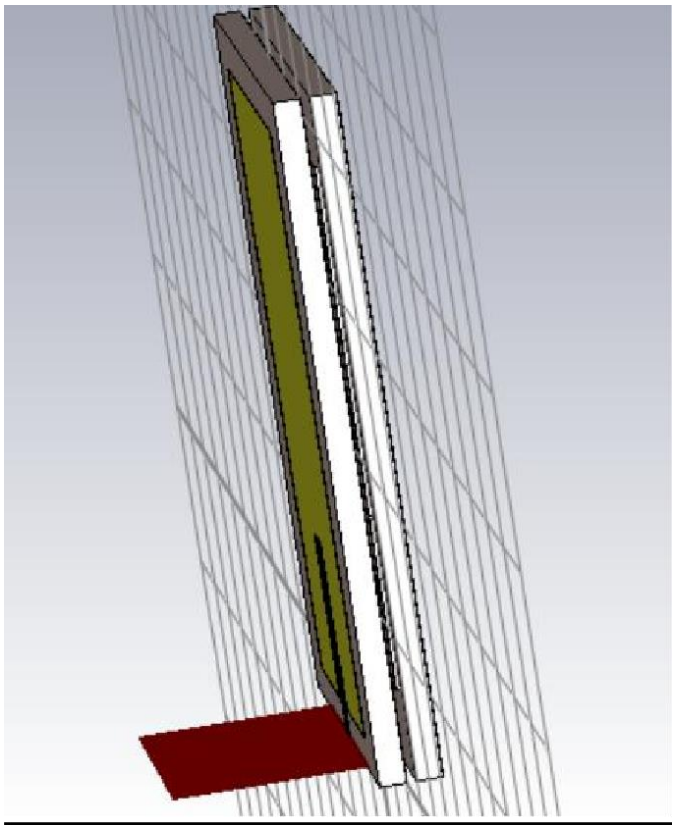

WORKING PRINCIPLE

- The **MTS unit cell** modifies the surrounding material's **permittivity (ε)** and **permeability (μ)**, enabling exotic behaviors such as **Zero-, High-, or Negative- Refractive Index** (ZRI, HRI, NRI), owing to its **sub-wavelength structure**.
- These features influence **transverse electromagnetic (EM) waves**, thereby altering the antenna's local **electromagnetic environment** when the MTS is integrated.
- Upon EM wave excitation:
    - The **resonant frequency** of the MTS is given by: **f_r = 1 / (2 * π * sqrt(L * C))** where **L** is inductance and **C** is capacitance of the unit cell.
- The **wavelength (λ)** in the substrate is: **λ = 300 / (f (in GHz) * sqrt(ε_r))** which affects resonance and radiation behavior.
- The antenna's **electric field** induces **voltage across ring gaps** in the MTS, generating **circulating currents**, which in turn create **magnetic fields**. This results in **resonance at 2.4 GHz** and forms an **effective high-refractive index (HRI)** region.
- The **effective patch dimensions** based on substrate permittivity and frequency are:
    - Effective Length (L_eff) = c / (2 * f_r * sqrt(1 / ε_r))
    - Effective Width (W_eff) = c / (2 * f_r * sqrt(ε_r))
- The interaction of MTS with the antenna modifies **effective ε and μ**, enabling:
    - Phase shifting
    - Amplitude modulation
    - Impedance matching

- These effects collectively enhance antenna performance by reducing reflection, improving energy transfer, and enabling better control of wave direction.

SIMULATION RESULTS

S PARAMETER

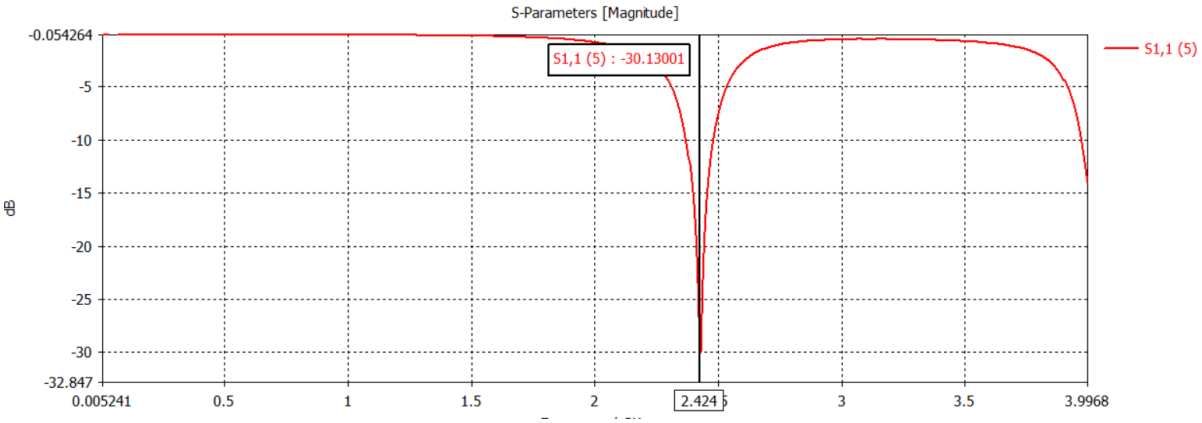

GAIN

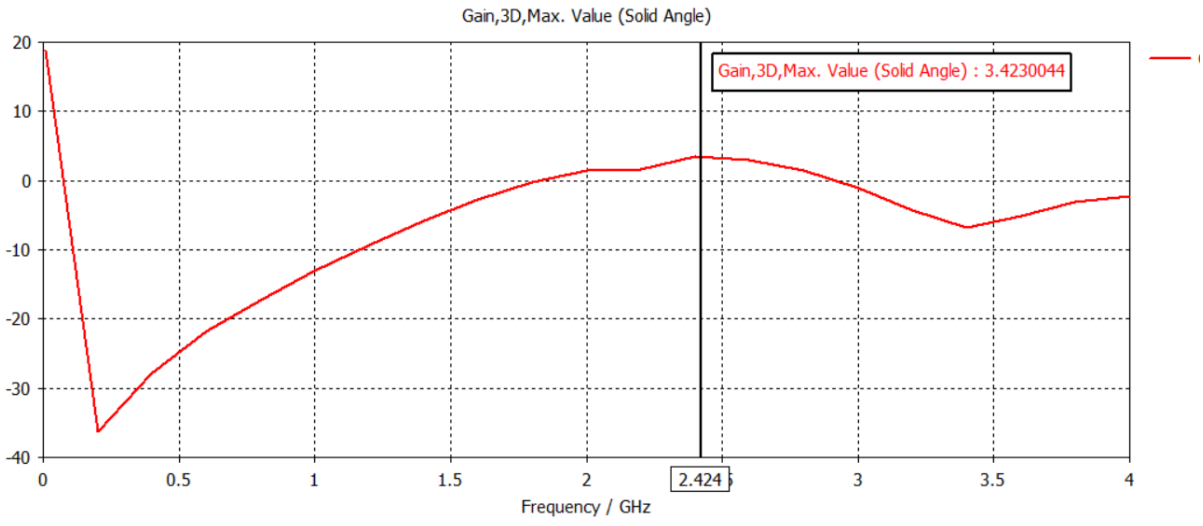

EFFICIENCY

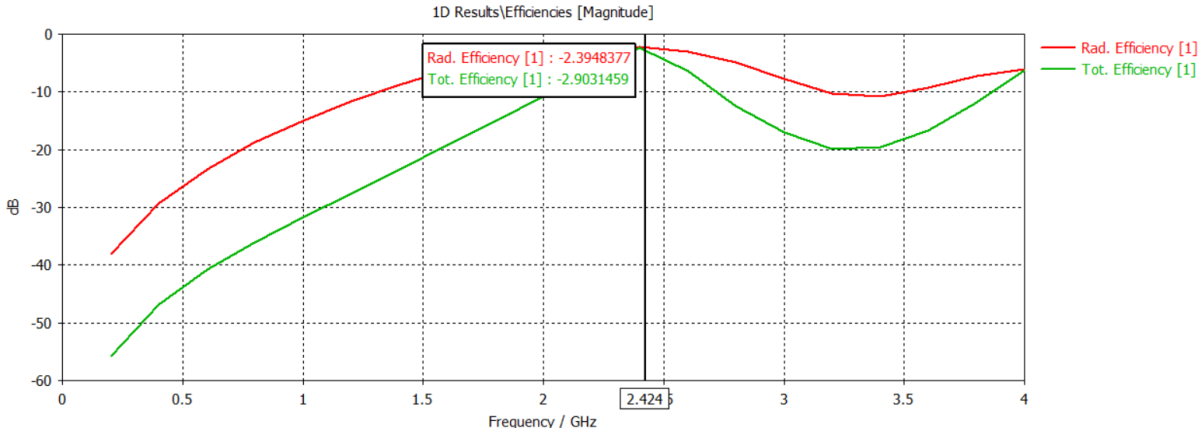

VSWR

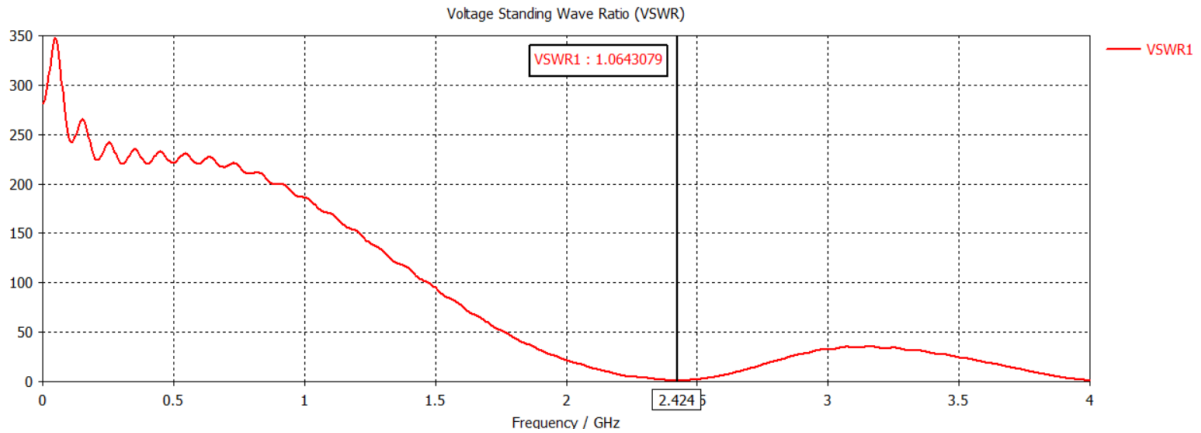

ACCEPTED POWER

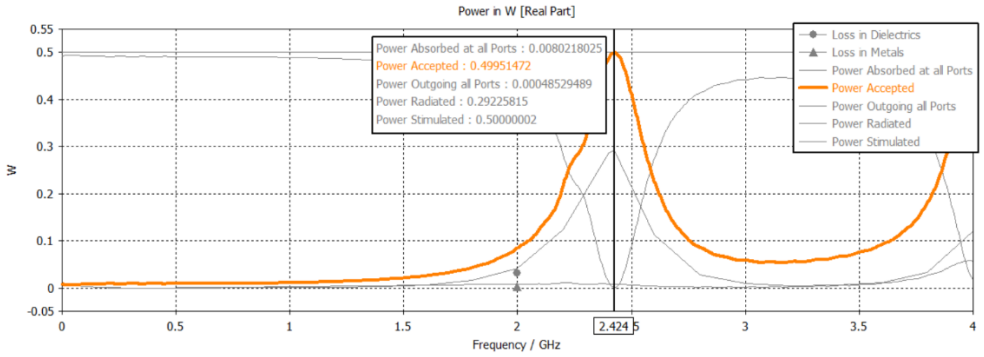

RADIATED POWER

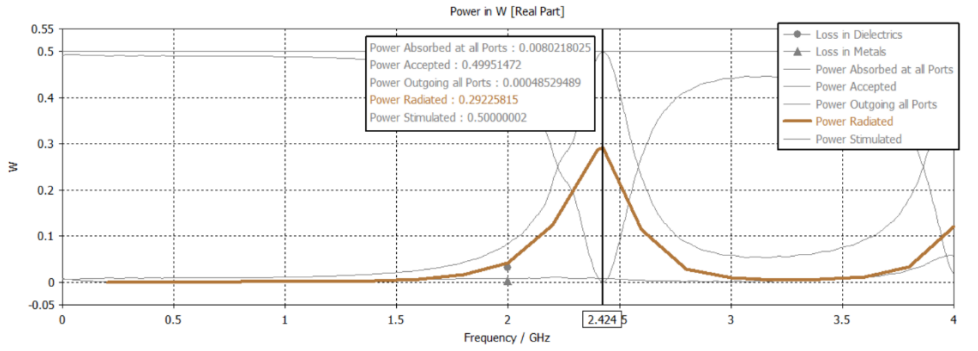

FAR FIELD

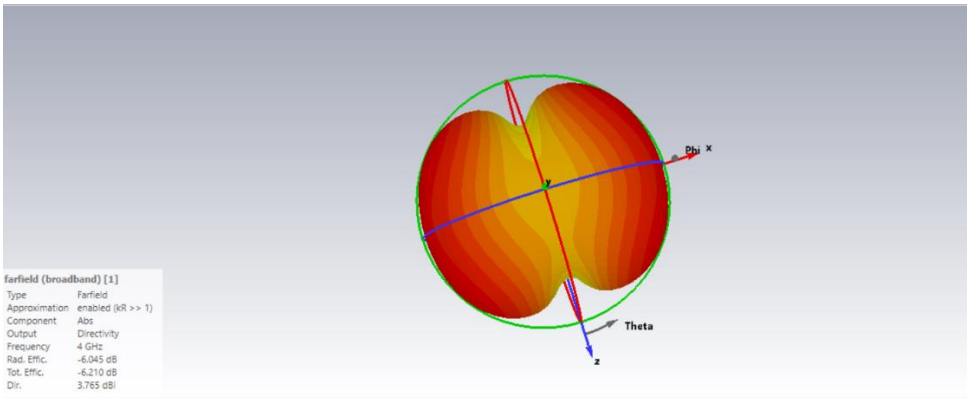

DIRECTIVITY

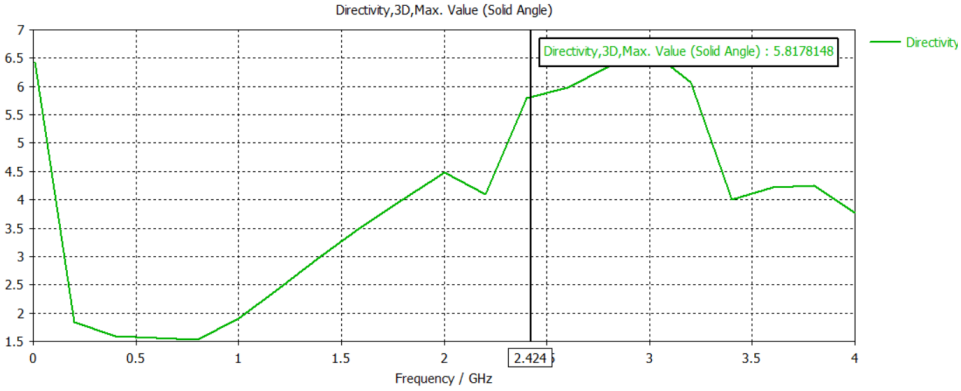

ANALYSIS:

CST Studio Suite was used to design and analyze the performance of the antenna and the metasurface (MTS). The desired resonance frequency for the unit cell was set at 2.4 GHz, and performance parameters were monitored across the 1 to 4 GHz frequency band.

1. **S11/ Return Loss:**

   Based on the simulated graphs, the resonant frequency was optimized to **2.024 GHz** in the final tuned design. After slightly adjusting the patch size, the MTS- integrated antenna demonstrated optimal performance at **2.424 GHz**. Notably, it achieved an S11 value of approximately **–30.13dB** at **2.424 GHz**, which indicates excellent impedance matching.

2. **Permittivity and Permeability:**

   Although an exact extraction of ε and μ was not conducted due to time constraints, an analytical estimate based on unit cell size and resonance frequency gives:

   $\varepsilon_{eff} \approx 30$ to 40, $\mu_{eff} \approx 1$ to 1.5 .

These values are consistent with typical high-index metasurfaces reported in literature and justify the observed improvements in gain, bandwidth, and impedance matching.

3. **Bandwidth:**

   Bandwidth is calculated as the frequency range where the return loss (S11) stays below –10 dB. In our design, this range was from approximately **2.33 GHz** to **2.535 GHz**, giving a total bandwidth of 205 MHz. This wide bandwidth is achieved due to the integration of the metasurface layer, which improves impedance matching over a broader range.

4. **Gain:**

   The antenna exhibits a **gain** of **3.42 dB** at the resonant frequency of **2.424 GHz**. This value reflects the combined effect of the antenna's ability to direct radiated energy and its efficiency. It indicates that the

antenna delivers moderate signal strength in the desired direction, which is good for compact, low-profile designs.

5. **Efficiency:**

   The antenna's **radiation efficiency** is **57.76%,** and **total efficiency** is **51.26%.** This means that more than half of the accepted power is successfully radiated, while the rest is lost due to dielectric losses (in FR4) and conductor losses. These values are acceptable given the use of lossy substrate and confirm the performance gain achieved through metasurface integration.

6. **VSWR:**

   The **Voltage Standing Wave Ratio (VSWR)** is **1.06**, which is extremely close to the ideal value of 1.0. This indicates **excellent impedance matching** between the antenna and the 50-ohm feed line, with minimal reflected power. Such a low VSWR ensures efficient power transfer and stable performance.

7. **Accepted and Radiated Power:**

   The antenna accepts **0.499 W** of power from the 1 W input source at 2.424 GHz. This means **49.9%** of the input power is actually delivered to the antenna for radiation, while the rest is reflected or lost in mismatch. It aligns well with the reported VSWR and S11 values.

   The **radiated power is 0.291 W**, which is the amount of input power successfully emitted as electromagnetic radiation. This confirms that the antenna is functioning effectively, with radiation losses kept under control through the metasurface's field-focusing behavior.

8. **Directivity**:

   At 2.424 GHz, the antenna demonstrates a **directivity of 5.82 dBi**, indicating its ability to concentrate energy in a specific direction. This value is enhanced due to the presence of the metasurface layer, which modifies the wavefront and suppresses backward radiation, improving forward gain and overall performance.

9. **Farfield:**

The farfield radiation pattern shows how the antenna radiates energy at a large distance, where the fields form stable wavefronts. In your design, the farfield pattern at 4 GHz is directional, with strong lobes in specific directions, indicating focused radiation. The plot confirms that the antenna maintains a symmetric and structured 3D pattern, supporting its use in point-to-point or directional wireless applications

COMPARISON TABLE

	PROPOSED DESIGN	OUR DESIGN
Frequency	2.4	2.424
|S11|	21.89 db	30.13 db
Gain	4.22 db	3.42 db
Efficiency	62%	57.76%

NOVELTY

The proposed design should achieve a reflection coefficient of 30.13 dBs at 2.4 gigahertz, which is significantly better than the values reported in paper 25, where the reflection coefficients were 12 dBs at 2 gHz and 18 dBs at 4.5 gHz. Additionally, at 2.4 gHz, the proposed antenna exhibits a gain of 3.42 decibels, outperforming the 1.3674 dbs gain reported in paper 24. The overall size of the proposed antenna is 0.352 times the free-space wavelength, which is considerably smaller than the 14 times free-space wavelength reported in paper 20. Moreover, the aperture efficiency of this antenna is 10 percent greater than the 30 percent efficiency mentioned in paper 23. The bandwidth has also increased from 123 mHz to 205 mHz, respectively. Compared to conventional designs, the integration of a metasurface with a microstrip patch antenna results in substantial enhancements in gain, bandwidth, efficiency, and radiation characteristics.

CONCLUSION

The design process and working mechanism of the resonant elements of metasurface and how it improves antenna performances in terms of impedance matching, bandwidth, gain, efficiency, and radiation profiles are discussed. The suggested antenna can be utilised for better conectivity in variety of devices (Wi-Fi routers, IOT, bluetooth devices, access points) and other wireless networking devices to enable high-speed data transfer and improved communication. These applications demonstrate the wide range of applications for the proposed antenna in the wireless and telecommunications industries, which have a significant impact on contemporary technology.

REFERENCES

- Le-Wei Li, Ya-Nan Li, Tat Soon Yeo, Juan R. Mosig, and Olivier J. F. Martin, "A broadband and high-gain Metamaterial microstrip antenna," *Applied Physics Letters*, vol. 96, no. 16, p. 164101, Apr. 2010.
- F. Araújo, A. L. P. S. Campos, R. V. De Andrade Lira, A. G. Neto, and A. G. D'Assunção, "Bandwidth enhancement of microstrip patch antenna using Metasurface," *Journal of Microwaves, Optoelectronics and Electromagnetic Applications*, vol. 20, no. 1, pp. 105–117, Mar. 2021.
- R. Garg, P. Bhartia, I. Bahl, and A. Ittipiboon, *Microstrip Antenna Design Handbook*, Artech House, Boston, MA, USA, Oct. 31, 2000.
- Indasen Singh and V. S. Tripathi, "Microstrip Patch Antenna and its Applications: a Survey," *International Journal of Computer and Applications in Technology*, vol. 2, no. 8, pp. 1595–1599, Sep. 2011.
- R. B. Rani, P. Kaur, and N. Verma, "Metamaterials and their applications in Patch Antenna: a review," *International Journal of Hybrid Information Technology*, vol. 8, no. 11, pp. 199–212, Nov. 2015.
- R. S. Kshetrimayum, "A brief intro to Metasurface," *IEEE Potentials*, vol. 23, no. 5, pp. 44–46, Jan. 2005.
- J. P. Deschamps, "Microstrip microwave antennas," *Proceedings of the IEEE*, vol. 55, no. 1, pp. 170–185, Jan. 1967, doi: 10.1109/PROC.1967.5214.
- X. Gao, Y. Zhang, and S. Li, "High Refractive Index Metasurface Superstrate for Microstrip Patch Antenna Performance Improvement," *Frontiers in Physics*, vol. 8, pp. 1–7, Sep. 2020.
- R. W. Ziolkowski and N. Engheta, "Metamaterials: Two decades past and into their Electromagnetics future Beyond," *IEEE Transactions on Antennas and Propagation*, vol. 68, no. 3, pp. 1232–1237, Mar. 2020.
- P. Kadam, P. Manikanta, and N. Rao, "Metasurface based microstrip patch antenna at 11GHz frequency for enhanced gain and directivity," *2022 1st International Conference on the Paradigm Shifts in Communication, Embedded Systems, Machine Learning and Signal Processing (PCEMS)*, Nagpur, India, 2022, pp. 88–92.
- Balanis, C. A., *Antenna Theory: Analysis and Design*, 4th ed., Hoboken: John Wiley & Sons, 2016.
- M. Saravanan, V. B. Geo, and S. Umarani, "Gain enhancement of patch antenna integrated with metamaterial inspired superstrate," *Journal of Electrical Systems and Information Technology*, vol. 5, no. 3, pp. 263–270, Dec. 2018.
- Z. Mahmud, M. T. Islam, N. Misran, M. J. Singh, and K. Mat, "A negative index metamaterial to enhance the performance of miniaturized UWB antenna for microwave imaging applications," *Applied Sciences*, vol. 7, no. 11, p. 1149, Nov. 2017.

- Md. Rashedul Islam et al., “Square enclosed circle split ring resonator enabled epsilon negative (ENG) near zero index (NZI) Metasurface for gain enhancement of multiband satellite and radar antenna applications,” *Results in Physics*, vol. 19, p. 103556, Dec. 2020.
- A. K. Singh, M. P. Abegaonkar, and S. K. Koul, “A negative index metamaterial lens for antenna gain enhancement,” *International Symposium on Antennas and Propagation (ISAP)*, Phuket, Thailand, Nov. 2017, pp. 1–2.
- N. Hussain et al., “A Metasurface-Based Low-Profile wideband circularly polarized patch antenna for 5G Millimeter-Wave systems,” *IEEE Access*, vol. 8, pp. 22127–22135, Jan. 2020.
- D. S. Sneha et al., “Non-Uniform Metasurface-Based Microstrip Patch Antenna With Bandwidth and Gain Enhancement for Wireless Applications,” *2023 International Conference on RAEEUCCI*, Chennai, India, 2023, pp. 1–4.
- S. Painam, V. S. Anumala, and M. Gatram, “Triple-Band Antenna for IoT and 5G Applications using Metasurfaces and Polygon Slot,” *2021 IEEE InCAP*, Jaipur, India, 2021, pp. 416–419.
- S. Ahmad et al., “A Metasurface-Based Single-Layered Compact AMC-Backed Dual Band Antenna for Off-Body IoT Devices,” *IEEE Access*, vol. 9, pp. 159598–159615.
- M. Koohestani and A. Ghaneizadeh, “An ultra-thin double functional metasurface patch antenna for UHF RFID applications,” *Scientific Reports*, vol. 11, no. 1, Jan. 2021.
- Komal Iqbal and Qasim Umar Khan, “Review of Metasurfaces Through Unit Cell Design and Numerical Extraction of Parameters and Their Applications in Antennas,” *IEEE Access*, vol. 10, pp. 112368–112391, Jan. 2022.
- Maalim Al-Abbasi and Tarik Abdul Latef, “Wideband circularly polarized fractal antenna with SSRR metasurface for 5G applications,” *International Journal of Electrical and Computer Engineering Systems*, vol. 15, no. 1, pp. 89–98, Jan. 2024.
- Gazali Bashir, Amit Kumar Singh, and Ankit Dubey, “Wide Band Beam Steering Digital Metasurface Reflectarray Antenna for Millimeter Wave Applications,” *IEEE Access*, vol. 11, pp. 121800–121810, Jan. 2023.
- Abdel-Ali Laabadli et al., “A miniaturized rectangular microstrip patch antenna with negative permeability unit cell metamaterial for the band 2.45 GHz,” *ITM Web of Conferences*, vol. 52, p. 03002, Jan. 2023.
- Nameeta Sharma, Kirti Vyas, and Rahul Srivastava, “A Comparative Study of Two Different Type of Metamaterial Unit Cells for Miniaturization and Multiband of Microstrip Patch Antenna at 2.4 GHz Frequency,” *IOP Conference Series: Earth and Environmental Science*, vol. 795, no. 1, p. 012020, Jun. 20

THANK YOU